

Generic shape of multichromatic resonance peaks

María Laura Olivera¹, Jesús Casado-Pascual¹, and Sigmund Kohler²

¹ Física Teórica, Universidad de Sevilla, Apartado de Correos 1065, 41080 Sevilla, Spain

² Instituto de Ciencia de Materiales de Madrid, CSIC, 28049 Madrid, Spain

December 5, 2021

Abstract. We investigate dissipative dynamical systems under the influence of an external driving with two or more frequencies. Our main quantities of interest are long-time averages of expectation values which turn out to exhibit universal features. In particular, resonance peaks in the vicinity of commensurable frequencies possess a generic enveloping function whose width is inversely proportional to the averaging time. While the universal features can be derived analytically, the transition from the specific short-time behavior to the long-time limit is illustrated for the examples of a classical random walk and a dissipative two-level system both with biharmonic driving. In these models, the dependence of the time-averaged response on the relative phase between the two driving frequencies changes with increasing integration time. For short times, it exhibits the 2π periodicity of the dynamic equations, while in the long-time limit, the period becomes a fraction of this value.

PACS.

1 Introduction

Dynamical systems driven by time-dependent forces represent paradigmatic models for non-equilibrium effects in the realm of both classical and quantum mechanics. There one may find counter-intuitive phenomena such as stochastic resonance [1, 2], synchronization [3–7], and the ratchet effect by which directed currents emerge despite the absence of any net force [8–10]. The common physics behind these phenomena is an interplay of non-linearities and non-equilibrium. Driven systems have been studied in the Hamiltonian limit [11–13], as well as in the steady state of dissipative classical [8, 9, 14, 15] and quantum mechanical models [16–18].

Even far from equilibrium, spatio-temporal symmetries may inhibit the emergence of a dc response such as a ratchet current. Many of these symmetries are based on the fact that a sinusoidal driving force changes its sign when time is shifted by half a period. For bichromatic or multichromatic forces, the periods of the various forces are different and, thus, the symmetry analysis has to be revised. Typically, one has to distinguish two cases, namely those of commensurable and incommensurable frequencies. In the former case, the symmetry depends on the phase between the components of the driving, which has been verified with transport experiments in quantum dots [19, 20]. In reference [19], it has also been demonstrated theoretically and experimentally that for incommensurable frequencies, the symmetry may be higher, despite that the driving force is only quasi periodic and may not possess any symmetry or anti-symmetry.

Here, we work out generic properties of dissipative dynamical systems under multi-frequency driving, in particular the shape of the resulting resonance peaks in the long-time limit. Moreover, we study how this limit emerges. The article is organized as follows. In Section 2, we formulate the problem and in Section 3 derive how the independence on the initial time provides generic properties. In Section 4, we consider finite-time effects for bichromatic driving and in Sections 5 and 6 show how the limits are approached for a classical random walk model and for a quantum mechanical two-level system, respectively. Finally, we summarize and conclude in Section 7.

2 Formulation of the problem

Suppose that the dynamical equations governing the time evolution of the system under consideration depend on time through N time-periodic functions of the form

$$f_j(t) = \Phi_j(\Omega_j t + \varphi_j), \quad (1)$$

with $j = 1, \dots, N$. In the above expression, Φ_j are 2π -periodic functions [i.e., $\Phi_j(\theta + 2\pi) = \Phi_j(\theta) \forall \theta \in \mathbb{R}$] and Ω_j and φ_j denote the angular frequency and the phase of $f_j(t)$, respectively. The precise nature of the functions $f_j(t)$ is irrelevant for our purposes, e.g., they may represent external oscillatory forces, modulating amplitudes, etc.

Assume that the system has been prepared in a state s_0 at an initial time t_0 . Depending on the case, s_0 may represent the system's density operator (in the case of quantum

systems), the one-time probability density (in the case of classical stochastic systems), the values of a finite number of state variables or classical fields (in the case of classical deterministic systems), etc. For our purpose, the only relevant fact is that all the physical properties of the system at any subsequent time $t \geq t_0$ are uniquely determined by this initial preparation and the dynamical equations. In particular, the (expectation) value at time $t \geq t_0$ of a certain physical quantity Q of this system, denoted by Q_t , will depend on the specific values taken by the parameters appearing in the functions $f_j(t)$, as well as, on the initial preparation. When necessary, this dependence will be made explicit by the notation $Q_t(\boldsymbol{\Omega}, \boldsymbol{\varphi}|_{s_0, t_0})$ with the vector notation $\boldsymbol{\Omega} = (\Omega_1, \dots, \Omega_N)$ and $\boldsymbol{\varphi} = (\varphi_1, \dots, \varphi_N)$.

The transformation property of $Q_t(\boldsymbol{\Omega}, \boldsymbol{\varphi}|_{s_0, t_0})$ is determined by the f_j , as for any time shift τ , the set of periodic functions $\{f_j(t)\}_{j=1, \dots, N}$ is invariant under the transformation $\{t, \boldsymbol{\varphi}\} \mapsto \{t + \tau, \boldsymbol{\varphi} - \boldsymbol{\Omega}\tau\}$. Consequently, since the only explicit time-dependence of the dynamical equations comes from the functions $f_j(t)$, it readily follows that

$$Q_t(\boldsymbol{\Omega}, \boldsymbol{\varphi}|_{s_0, t_0}) = Q_{t+\tau}(\boldsymbol{\Omega}, \boldsymbol{\varphi} - \boldsymbol{\Omega}\tau|_{s_0, t_0 + \tau}). \quad (2)$$

In particular, taking $\tau = -t$, one obtains

$$Q_t(\boldsymbol{\Omega}, \boldsymbol{\varphi}|_{s_0, t_0}) = Q_0(\boldsymbol{\Omega}, \boldsymbol{\varphi} + \boldsymbol{\Omega}t|_{s_0, t_0 - t}). \quad (3)$$

Henceforth, we assume that, after a certain transient time (or, more formally, in the limit $t_0 \rightarrow -\infty$), the observable under investigation reaches a stationary value

$$Q_t^{\text{st}}(\boldsymbol{\Omega}, \boldsymbol{\varphi}) = \lim_{t_0 \rightarrow -\infty} Q_t(\boldsymbol{\Omega}, \boldsymbol{\varphi}|_{s_0, t_0}). \quad (4)$$

This assumption has been found in many dissipative systems. From equation (3), it then follows that

$$Q_t^{\text{st}}(\boldsymbol{\Omega}, \boldsymbol{\varphi}) = Q_0^{\text{st}}(\boldsymbol{\Omega}, \boldsymbol{\varphi} + \boldsymbol{\Omega}t). \quad (5)$$

Therefore, in the stationary regime, the time evolution of Q admits a description in terms of a time-dependent phase vector of the form $\boldsymbol{\varphi} + \boldsymbol{\Omega}t$.

Here, we are interested in the generic properties of the time average

$$\overline{Q}_T(\boldsymbol{\Omega}, \boldsymbol{\varphi}) = \frac{1}{T} \int_0^T dt Q_t^{\text{st}}(\boldsymbol{\Omega}, \boldsymbol{\varphi}), \quad (6)$$

and more specifically on the infinite-time average

$$\overline{Q}_\infty(\boldsymbol{\Omega}, \boldsymbol{\varphi}) = \lim_{T \rightarrow \infty} \overline{Q}_T(\boldsymbol{\Omega}, \boldsymbol{\varphi}). \quad (7)$$

Since the functions $\Phi_j(\Omega_j t + \varphi_j)$ are 2π -periodic in the phases φ_j , so will be $Q_t^{\text{st}}(\boldsymbol{\Omega}, \boldsymbol{\varphi})$. Therefore, taking into account equation (5), it can be Fourier expanded as

$$Q_t^{\text{st}}(\boldsymbol{\Omega}, \boldsymbol{\varphi}) = \sum_{\mathbf{k} \in \mathbb{Z}^N} q_{\mathbf{k}}(\boldsymbol{\Omega}) e^{i\mathbf{k} \cdot (\boldsymbol{\varphi} + \boldsymbol{\Omega}t)}, \quad (8)$$

where the centered dot denotes the usual scalar product in \mathbb{R}^N and

$$q_{\mathbf{k}}(\boldsymbol{\Omega}) = \int_{-\pi}^{\pi} \cdots \int_{-\pi}^{\pi} \frac{e^{-i\mathbf{k} \cdot \boldsymbol{\varphi}}}{(2\pi)^N} Q_0^{\text{st}}(\boldsymbol{\Omega}, \boldsymbol{\varphi}) d^N \boldsymbol{\varphi}. \quad (9)$$

By inserting equation (8) into equation (6), we obtain

$$\overline{Q}_T(\boldsymbol{\Omega}, \boldsymbol{\varphi}) = \sum_{\mathbf{k} \in \mathbb{Z}^N} q_{\mathbf{k}}(\boldsymbol{\Omega}) e^{i\mathbf{k} \cdot (\boldsymbol{\varphi} + \boldsymbol{\Omega}T/2)} \text{sinc}\left(\frac{\mathbf{k} \cdot \boldsymbol{\Omega}T}{2}\right), \quad (10)$$

where $\text{sinc}(x) = \sin(x)/x$ denotes the unnormalized sinus cardinalis. Since $\lim_{T \rightarrow \infty} \text{sinc}(\alpha T/2)$ equals 1 if $\alpha = 0$ and 0 otherwise, from equations (7) and (10) we get

$$\overline{Q}_\infty(\boldsymbol{\Omega}, \boldsymbol{\varphi}) = \sum_{\mathbf{k} \in \mathcal{S}_\boldsymbol{\Omega}} q_{\mathbf{k}}(\boldsymbol{\Omega}) e^{i\mathbf{k} \cdot \boldsymbol{\varphi}}, \quad (11)$$

where $\mathcal{S}_\boldsymbol{\Omega}$ is the set of all ordered N -tuples of integers orthogonal to $\boldsymbol{\Omega}$, i.e., $\mathcal{S}_\boldsymbol{\Omega} = \{\mathbf{k} \in \mathbb{Z}^N : \mathbf{k} \cdot \boldsymbol{\Omega} = 0\}$.

If the N components of the frequency vector $\boldsymbol{\Omega}$ are incommensurable (i.e., it is not possible to express one of them as a linear combination of the others with rational coefficients), then the set $\mathcal{S}_\boldsymbol{\Omega}$ reduces to the single element $\mathbf{k} = \mathbf{0}$. In this case, from equation (11), it readily follows that

$$\overline{Q}_\infty(\boldsymbol{\Omega}, \boldsymbol{\varphi}) = q_0(\boldsymbol{\Omega}) \quad (12)$$

and, therefore, the infinite-time average is independent of $\boldsymbol{\varphi}$. An experimental verification of this general statement has been reported in reference [19].

In contrast, if the N components of $\boldsymbol{\Omega}$ are commensurable (i.e., it is possible to express one of them as a linear combination of the others with rational coefficients), then the set $\mathcal{S}_\boldsymbol{\Omega}$ contains additional elements other than $\mathbf{k} = \mathbf{0}$ and, according to equation (11), $\overline{Q}_\infty(\boldsymbol{\Omega}, \boldsymbol{\varphi})$ depends on the phases in $\boldsymbol{\varphi}$. In particular, if the frequencies are pairwise commensurable, then there exists a frequency Ω such that $\boldsymbol{\Omega} = \Omega \mathbf{n}$, where $\mathbf{n} = (n_1, \dots, n_N)$, with n_j being positive integers. Consequently, the condition $\mathbf{k} \cdot \boldsymbol{\Omega} = 0$ becomes equivalent to the Diophantine equation $\mathbf{k} \cdot \mathbf{n} = 0$. The general solution of the latter equation can be expressed as an integer linear combination of a set of $N - 1$ generating vectors, $\mathbf{g}^{(1)}, \dots, \mathbf{g}^{(N-1)}$, each of which satisfies the equation $\mathbf{g}^{(j)} \cdot \mathbf{n} = 0$ [15, 21, 22]. Thus, equation (11) can be written as

$$\overline{Q}_\infty(\boldsymbol{\Omega}, \boldsymbol{\varphi}) = \sum_{\boldsymbol{\ell} \in \mathbb{Z}^{N-1}} q_{\mathbf{k}(\boldsymbol{\ell})}(\boldsymbol{\Omega}) e^{i\mathbf{k}(\boldsymbol{\ell}) \cdot \boldsymbol{\varphi}}, \quad (13)$$

where $\mathbf{k}(\boldsymbol{\ell}) = \sum_{j=1}^{N-1} \ell_j \mathbf{g}^{(j)}$.

Let \mathcal{W}_C and \mathcal{W}_I be the sets of all $\boldsymbol{\Omega}$ whose components are commensurable and incommensurable, respectively. From the above results, it can easily be shown that the infinite-time average $\overline{Q}_\infty(\boldsymbol{\Omega}, \boldsymbol{\varphi})$ is discontinuous on the set \mathcal{W}_C . Indeed, since the set \mathcal{W}_I is dense in \mathbb{R}^N , for any $\boldsymbol{\Omega}_c \in \mathcal{W}_C$ one can find a sequence $\{\boldsymbol{\Omega}^{(n)}\}_{n \in \mathbb{N}} \subset \mathcal{W}_I$ such that $\lim_{n \rightarrow \infty} \boldsymbol{\Omega}^{(n)} = \boldsymbol{\Omega}_c$. If $\overline{Q}_\infty(\boldsymbol{\Omega}, \boldsymbol{\varphi})$ were continuous at $\boldsymbol{\Omega}_c$, then

$$\overline{Q}_\infty(\boldsymbol{\Omega}_c, \boldsymbol{\varphi}) = \lim_{n \rightarrow \infty} \overline{Q}_\infty(\boldsymbol{\Omega}^{(n)}, \boldsymbol{\varphi}) = \lim_{n \rightarrow \infty} q_0(\boldsymbol{\Omega}^{(n)}) \quad (14)$$

and, as a result, $\overline{Q}_\infty(\boldsymbol{\Omega}_c, \boldsymbol{\varphi})$ would be independent of $\boldsymbol{\varphi}$. Obviously, this contradicts the fact that, since $\boldsymbol{\Omega}_c \in \mathcal{W}_C$, $\overline{Q}_\infty(\boldsymbol{\Omega}_c, \boldsymbol{\varphi})$ depends on $\boldsymbol{\varphi}$. Hence, we can conclude that

$\overline{Q}_\infty(\boldsymbol{\Omega}, \varphi)$ is discontinuous at $\boldsymbol{\Omega}_c$ and, thus, on the set \mathcal{W}_C . Taking into account that \mathcal{W}_C is also dense in \mathbb{R}^N , this last result implies that the infinite-time average $\overline{Q}_\infty(\boldsymbol{\Omega}, \varphi)$ is a highly discontinuous function of the frequency vector $\boldsymbol{\Omega}$. In this context, the following questions arise: (i) Can this discontinuity actually be observed? (ii) How does it manifest itself in practice?

3 Long-time asymptotic behavior of \overline{Q}_T

In real situations, the physical quantity Q is known only in a finite time-interval. Therefore, the infinite time-average \overline{Q}_∞ can be calculated only approximately by taking a sufficiently large value of T . Suppose we are interested in analyzing the dependence of \overline{Q}_T on $\boldsymbol{\Omega}$ near a fixed frequency vector $\boldsymbol{\Omega}_0$. More precisely, we focus on values of $\boldsymbol{\Omega}$ such that $|\boldsymbol{\Omega} - \boldsymbol{\Omega}_0|$ is of the same order of magnitude as T^{-1} , where $|\boldsymbol{\Omega} - \boldsymbol{\Omega}_0| = [\sum_{j=1}^N (\Omega_j - \Omega_{0,j})^2]^{1/2}$. Then, as T increases, the size of the region of interest becomes smaller in inverse proportion to T .

By defining the dimensionless frequency vector $\delta\tilde{\boldsymbol{\omega}} = (\boldsymbol{\Omega} - \boldsymbol{\Omega}_0)T$, the finite time-average can be brought to the form

$$\begin{aligned} \overline{Q}_T(\boldsymbol{\Omega}, \varphi) &= \overline{Q}_T(\boldsymbol{\Omega}_0 + \delta\tilde{\boldsymbol{\omega}}/T, \varphi) \\ &= \overline{Q}_{\text{as}}(\boldsymbol{\Omega}_0, \delta\tilde{\boldsymbol{\omega}}, \varphi) + R_T(\boldsymbol{\Omega}_0, \delta\tilde{\boldsymbol{\omega}}, \varphi), \end{aligned} \quad (15)$$

where

$$\overline{Q}_{\text{as}}(\boldsymbol{\Omega}_0, \delta\tilde{\boldsymbol{\omega}}, \varphi) = \lim_{T \rightarrow \infty} \overline{Q}_T(\boldsymbol{\Omega}_0 + \delta\tilde{\boldsymbol{\omega}}/T, \varphi) \quad (16)$$

is the leading-order of the asymptotic behavior of the function $\overline{Q}_T(\boldsymbol{\Omega}_0 + \delta\tilde{\boldsymbol{\omega}}/T, \varphi)$ for $T \rightarrow \infty$, while $\delta\tilde{\boldsymbol{\omega}}$ is held constant. For the rest $R_T(\boldsymbol{\Omega}_0, \delta\tilde{\boldsymbol{\omega}}, \varphi) = \overline{Q}_T(\boldsymbol{\Omega}_0 + \delta\tilde{\boldsymbol{\omega}}/T, \varphi) - \overline{Q}_{\text{as}}(\boldsymbol{\Omega}_0, \delta\tilde{\boldsymbol{\omega}}, \varphi)$, it readily follows that

$$\lim_{T \rightarrow \infty} R_T(\boldsymbol{\Omega}_0, \delta\tilde{\boldsymbol{\omega}}, \varphi) = 0, \quad (17)$$

and together with equation (7), that

$$\overline{Q}_{\text{as}}(\boldsymbol{\Omega}_0, \mathbf{0}, \varphi) = \overline{Q}_\infty(\boldsymbol{\Omega}_0, \varphi). \quad (18)$$

To obtain an expression for $\overline{Q}_{\text{as}}(\boldsymbol{\Omega}_0, \delta\tilde{\boldsymbol{\omega}}, \varphi)$, we set $\boldsymbol{\Omega} = \boldsymbol{\Omega}_0 + \delta\tilde{\boldsymbol{\omega}}/T$ in equation (10), and insert the resulting expression into equation (16). Then, using again $\lim_{T \rightarrow \infty} \text{sinc}(\alpha T/2) = \delta_{\alpha,0}$, one obtains

$$\overline{Q}_{\text{as}}(\boldsymbol{\Omega}_0, \delta\tilde{\boldsymbol{\omega}}, \varphi) = \sum_{\mathbf{k} \in \mathcal{S}_\Omega} q_{\mathbf{k}}(\boldsymbol{\Omega}_0) e^{i\mathbf{k} \cdot (\varphi + \delta\tilde{\boldsymbol{\omega}}/2)} \text{sinc}\left(\frac{\mathbf{k} \cdot \delta\tilde{\boldsymbol{\omega}}}{2}\right). \quad (19)$$

Using equation (11), one sees that equation (19) can be written in the more compact form

$$\overline{Q}_{\text{as}}(\boldsymbol{\Omega}_0, \delta\tilde{\boldsymbol{\omega}}, \varphi) = \int_0^1 d\lambda \overline{Q}_\infty(\boldsymbol{\Omega}_0, \varphi + \lambda \delta\tilde{\boldsymbol{\omega}}). \quad (20)$$

Therefore, in the limit $T \rightarrow \infty$, the asymptotic behavior of \overline{Q}_T in a neighborhood of $\boldsymbol{\Omega}_0$ of size proportional to

T^{-1} is completely determined by the infinite-time limit \overline{Q}_∞ at $\boldsymbol{\Omega}_0$. Notice that, according to the above results, no matter how large T , it is always possible to find a neighborhood of $\boldsymbol{\Omega}_0$ within which \overline{Q}_T is continuous. Thus, the discontinuity mentioned in the previous section is a mathematical idealization that, owing to the necessarily finite measurement time, cannot be observed in reality.

From equation (20) there immediately follows an interesting conclusion. If $\boldsymbol{\Omega}_0 \in \mathcal{W}_I$ (i.e., all N components are incommensurable), then $\overline{Q}_\infty(\boldsymbol{\Omega}_0, \varphi)$ is independent of φ and $\overline{Q}_{\text{as}}(\boldsymbol{\Omega}_0, \delta\tilde{\boldsymbol{\omega}}, \varphi) = \overline{Q}_\infty(\boldsymbol{\Omega}_0, \varphi)$ for all $\delta\tilde{\boldsymbol{\omega}}$. Consequently, from equations (7) and (16), one obtains that

$$\lim_{T \rightarrow \infty} [\overline{Q}_T(\boldsymbol{\Omega}_0 + \delta\tilde{\boldsymbol{\omega}}/T, \varphi) - \overline{Q}_T(\boldsymbol{\Omega}_0, \varphi)] = 0 \quad (21)$$

for all $\delta\tilde{\boldsymbol{\omega}}$. In contrast, if $\boldsymbol{\Omega}_0 \in \mathcal{W}_C$ (i.e., its N components are commensurable), then $\overline{Q}_\infty(\boldsymbol{\Omega}_0, \varphi)$ depends on φ and, in general,

$$\lim_{T \rightarrow \infty} [\overline{Q}_T(\boldsymbol{\Omega}_0 + \delta\tilde{\boldsymbol{\omega}}/T, \varphi) - \overline{Q}_T(\boldsymbol{\Omega}_0, \varphi)] \neq 0. \quad (22)$$

This difference in behavior will be apparent in the numerical calculations presented below.

4 Bichromatic driving

The analytic considerations made so far provide the long-time limit of the non-linear response to a multi-frequency forcing. In order to investigate numerically how this limit is approached, we focus on bichromatic driving, i.e., on dynamic equations which contain terms of the form $f_1(t) = A_1 \cos(\Omega_1 t + \varphi_1)$ and $f_2(t) = A_2 \cos(\Omega_2 t + \varphi_2)$, where our line of reasoning still holds if the cosines are replaced by any other 2π -periodic functions.

4.1 Commensurable frequencies and periodicity in φ

While the 2π -periodicity of $\{f_1(t), f_2(t)\}$ in φ_1 and φ_2 is evident, discrete time translation symmetry is present only when Ω_1 and Ω_2 are commensurable, i.e., for rational values of Ω_2/Ω_1 . Indeed, let us assume that $f_1(t)$ and $f_2(t)$ have a common fundamental period \mathcal{T} . From the periodicity of the cosine function, it then follows that there must exist two integers q and p such that $\Omega_1 \mathcal{T} = 2\pi q$ and $\Omega_2 \mathcal{T} = 2\pi p$. This implies that $\Omega_1 = q\Omega$ and $\Omega_2 = p\Omega$, with $\Omega = 2\pi/\mathcal{T}$, and consequently, that $\Omega_2/\Omega_1 = p/q$. In addition, the integers q and p must be coprime because otherwise $\mathcal{T}/\text{gcd}(q, p) < \mathcal{T}$, would be the common fundamental period of $f_1(t)$ and $f_2(t)$, with $\text{gcd}(q, p)$ denoting the greatest common divisor of q and p .

Let us now focus on a frequency vector $\boldsymbol{\Omega}_0 \equiv (q, p)\Omega$, with some coprime integers p and q , henceforth referred to as (q, p) -resonance. Using equation (8), it can easily be seen that the stationary value $Q_i^{\text{st}}(\boldsymbol{\Omega}_0, \varphi)$ is a \mathcal{T} -periodic function of time. A further interesting fact is that the infinite-time average $\overline{Q}_\infty(\boldsymbol{\Omega}_0, \varphi)$ displays a higher symmetry in φ than the obvious $\varphi_1 \rightarrow \varphi_1 + 2\pi$ and $\varphi_2 \rightarrow$

$\varphi_2 + 2\pi$ [14]. To see that this is so, note that in the present case the condition $\mathbf{k} \cdot \boldsymbol{\Omega}_0 = 0$ becomes equivalent to $k_1 q + k_2 p = 0$. The general solution of this Diophantine equation is $\ell \mathbf{g}$, with the generating vector $\mathbf{g} \equiv (-p, q)$ and any integer ℓ . Thus, in this case, equation (13) becomes

$$\overline{Q}_\infty(\boldsymbol{\Omega}_0, \varphi) = \sum_{\ell \in \mathbb{Z}} q_{\ell \mathbf{g}}(\boldsymbol{\Omega}_0) e^{i \ell \mathbf{g} \cdot \varphi}. \quad (23)$$

Since $\mathbf{g} \cdot \varphi = -p\varphi_1 + q\varphi_2$, from equation (23) it readily follows that $\overline{Q}_\infty(\boldsymbol{\Omega}_0, \varphi)$ is $2\pi/p$ -periodic in φ_1 and $2\pi/q$ -periodic in φ_2 .

4.2 The neighborhood of commensurable frequencies

Let us now turn our attention to the vicinity of a (q, p) -resonance. More specifically, and following the general approach outlined in Section 3, we focus on values of $\boldsymbol{\Omega}$ such that $|\boldsymbol{\Omega} - \boldsymbol{\Omega}_0| = [(\Omega_1 - q\Omega)^2 + (\Omega_2 - p\Omega)^2]^{1/2}$ is of the same order as T^{-1} . Then, introducing the notation $\delta\boldsymbol{\omega} = \delta\tilde{\boldsymbol{\omega}}/T = \boldsymbol{\Omega} - \boldsymbol{\Omega}_0$, from equation (15), (17), and (19), it follows that

$$\overline{Q}_T(\boldsymbol{\Omega}_0 + \delta\boldsymbol{\omega}, \varphi) \sim \sum_{\ell \in \mathbb{Z}} q_{\ell \mathbf{g}}(\boldsymbol{\Omega}_0) e^{i \ell \mathbf{g} \cdot (\varphi + T\delta\boldsymbol{\omega}/2)} \times \text{sinc}\left(\frac{\ell T \mathbf{g} \cdot \delta\boldsymbol{\omega}}{2}\right), \quad (24)$$

provided that T is large enough so that the term R_T can be neglected.

Two conclusions can be drawn from equation (24). First, the time average $\overline{Q}_T(\boldsymbol{\Omega}_0 + \delta\boldsymbol{\omega}, \varphi)$ is $2\pi/p$ -periodic in φ_1 and $2\pi/q$ -periodic in φ_2 . There is, however, an important difference to the exact periodicity of the infinite-time average $\overline{Q}_\infty(\boldsymbol{\Omega}_0, \varphi)$ presented in Section 4.1. Here the periodicity holds only for sufficiently large values of T and for $\boldsymbol{\Omega}$ sufficiently close to $\boldsymbol{\Omega}_0$ —to be precise, for $|\delta\boldsymbol{\omega}| = \mathcal{O}(T^{-1})$. Second, under these same restrictions, the relative height $\Delta\overline{Q}_T(\boldsymbol{\Omega}_0 + \delta\boldsymbol{\omega}, \varphi) \equiv \overline{Q}_T(\boldsymbol{\Omega}_0 + \delta\boldsymbol{\omega}, \varphi) - q_0(\boldsymbol{\Omega}_0)$ vanishes when all sinc functions in equation (24) are zero for all $\ell \neq 0$, i.e., when $\mathbf{g} \cdot \delta\boldsymbol{\omega}$ is a nonzero integer multiple of $2\pi/T$. In particular, if we set $\delta\omega_1 = 0$ and vary $\delta\omega_2$, $\Delta\overline{Q}_T(\boldsymbol{\Omega}_0 + \delta\boldsymbol{\omega}, \varphi)$ vanishes when $\delta\omega_2$ is a nonzero integer multiple of $2\pi/(qT)$. Analogously, if we set $\delta\omega_2 = 0$ and vary $\delta\omega_1$, $\Delta\overline{Q}_T(\boldsymbol{\Omega}_0 + \delta\boldsymbol{\omega}, \varphi)$ vanishes when $\delta\omega_1$ is a nonzero integer multiple of $2\pi/(pT)$. Hence, in the vicinity of the (q, p) -resonance, $2\pi/(qT)$ and $2\pi/(pT)$ represent the frequency scales on which $\Delta\overline{Q}_T(\boldsymbol{\Omega}_0 + \delta\boldsymbol{\omega}, \varphi)$ varies.

The main aim of the next two sections is to provide quantitative information on how these asymptotic properties can actually be observed in practice. Note, for example, that a further limitation may stem from the fact that the set of commensurable frequencies vectors is dense in \mathbb{R}^2 and, consequently, any (q, p) -resonance may be disturbed by another resonance that lies arbitrarily close to it. It will turn out, however, for all cases investigated, practically only resonances with rather small q and p matter. Moreover, for sufficiently large values of T , the shape of

the resonance peak is mainly governed by the term with $\ell = 1$ in equation (24) and, therefore, their enveloping function appears as a rather clean sinc function.

5 Classical random walk model

In the model presented in this section, the motion of a particle in a periodic substrate is given by a random walk on a one-dimensional lattice. The lattice sites are located at $x_n = na$, where n is any integer and a the distance between two neighboring sites. The evolution of the probabilities $p_n(t)$ that the particle is at site n is governed by the master equation [23]

$$\dot{p}_n(t) = -[r_+(t) + r_-(t)]p_n(t) + r_+(t)p_{n-1}(t) + r_-(t)p_{n+1}(t), \quad (25)$$

where $r_+(t)$ and $r_-(t)$ are the transition rates from site n to site $n+1$ and $n-1$, respectively. They are assumed to be independent of n and to follow the Van't Hoff-Arrhenius law [24]

$$r_\pm(t) = r_0 e^{-\beta[E_0 \pm \Delta E(t)]}, \quad (26)$$

where r_0 is a prefactor with the dimension of an inverse time, $\beta = (k_B\Theta)^{-1}$ is the inverse temperature, and $E_0 + \Delta E(t)$ and $E_0 - \Delta E(t)$ are, respectively, the activation energies for the forward and backward steps. These activation energies oscillate around a constant value E_0 with time-dependent amplitudes $\Delta E(t)$ and $-\Delta E(t)$, respectively.

In this section, we will consider that the role of Q_t is played by the mean particle velocity V_t , which is defined as the time derivative of the mean particle position $X_t = a \sum_{n \in \mathbb{Z}} n p_n(t)$. Using equations (25) and (26), it can be seen easily that

$$V_t = a[r_+(t) - r_-(t)] = v \sinh[f(t)], \quad (27)$$

where $v = 2ar_0 e^{-\beta E_0}$ and $f(t) = -\beta \Delta E(t)$. Henceforth, we will assume that

$$f(t) = A_1 \cos(\Omega_1 t + \varphi_1) + A_2 \cos(\Omega_2 t + \varphi_2), \quad (28)$$

with A_1 and A_2 being two dimensionless constants, which can be taken as positive by suitable choice of the phases φ_1 and φ_2 . Note that, in the present model, there is no difference between the stationary V_t^{st} and V_t because the mean particle velocity is independent of the initial preparation. In addition, from equations (27) and (28), it immediately follows that V_t satisfies the symmetry properties

$$V_{-t}(\boldsymbol{\Omega}, -\varphi) = V_t(\boldsymbol{\Omega}, \varphi), \quad (29)$$

$$V_t(\boldsymbol{\Omega}, \varphi + \boldsymbol{\pi}) = -V_t(\boldsymbol{\Omega}, \varphi), \quad (30)$$

where $\boldsymbol{\pi} \equiv (\pi, \pi)$.

Now the Fourier expansion in equation (8) takes the form

$$V_t(\boldsymbol{\Omega}, \varphi) = \sum_{\mathbf{k} \in \mathbb{Z}^2} v_{\mathbf{k}} e^{i \mathbf{k} \cdot (\varphi + \boldsymbol{\Omega} t)}, \quad (31)$$

with

$$v_{\mathbf{k}} = v \int_{-\pi}^{\pi} \int_{-\pi}^{\pi} \frac{e^{-i\mathbf{k}\cdot\boldsymbol{\varphi}}}{(2\pi)^2} \sinh(A_1 \cos \varphi_1 + A_2 \cos \varphi_2) d^2\boldsymbol{\varphi}. \quad (32)$$

Since the Fourier expansion is unique, using equations (29) and (31), it is easy to see that $v_{-\mathbf{k}} = v_{\mathbf{k}}$. For the same reason, from equations (30) and (31), it readily follows that $v_{\mathbf{k}} = -e^{i(k_1+k_2)\pi} v_{\mathbf{k}}$. In addition, from equation (32), it is clear that $v_{\mathbf{k}}^* = v_{-\mathbf{k}}$, where the asterisk denotes complex conjugation. In conclusion, all the coefficients $v_{\mathbf{k}}$ are real and vanish when $k_1 + k_2$ is an even integer.

With the above results, let us now examine the dependence of the infinite-time average velocity on $\boldsymbol{\Omega}$. If Ω_1 and Ω_2 are incommensurable, from equation (12) one concludes that $\bar{V}_{\infty}(\boldsymbol{\Omega}, \boldsymbol{\varphi}) = v_0 = 0$. If, by contrast, Ω_1 and Ω_2 are commensurable, taking into account that $v_{\mathbf{k}} = v_{-\mathbf{k}}$ and that $v_{2\mathbf{k}} = 0$, it is easy to see from equation (23) that

$$\bar{V}_{\infty}(\boldsymbol{\Omega}_0, \boldsymbol{\varphi}) = 2 \sum_{\ell=0}^{\infty} v_{(2\ell+1)\mathbf{g}} \cos[(2\ell+1)\mathbf{g} \cdot \boldsymbol{\varphi}]. \quad (33)$$

Using the definition of \mathbf{g} and the fact that $v_{\mathbf{k}}$ vanishes when $k_1 + k_2$ is even, it can be verified with equation (33) that $\bar{V}_{\infty}(\boldsymbol{\Omega}_0, \boldsymbol{\varphi}) = 0$ when $q - p$ is even. Therefore, as a consequence of the symmetry property (30), only the (q, p) -resonances with $q - p$ odd are present in this model.

The integral in equation (32) can be evaluated explicitly by expanding the hyperbolic sine into a power series. Then, after some calculations, we obtain

$$v_{\mathbf{k}} = v \sum_{j=0}^{\infty} \sum_{\ell=0}^{2j+1} \sum_{m=0}^{\ell} \sum_{n=0}^{2j+1-\ell} \delta_{k_1, 2m-\ell} \delta_{k_2, 2n+\ell-2j-1} \times \frac{A_1^{\ell} A_2^{2j+1-\ell}}{2^{2j+1} m! n! (\ell-m)! (2j+1-\ell-n)!}. \quad (34)$$

It can be verified that the coefficients $v_{\mathbf{k}}$ given by equation (34), as could not be otherwise, satisfy the conditions discussed above. In addition, since A_1 and A_2 are positive, all the coefficients $v_{\mathbf{k}}$ are clearly non-negative. Thus, from equation (33), it follows that the maximum value of $\bar{V}_{\infty}(\boldsymbol{\Omega}_0, \boldsymbol{\varphi})$ is

$$\bar{V}_{\infty, \text{M}}(\boldsymbol{\Omega}_0) = 2 \sum_{\ell=0}^{\infty} v_{(2\ell+1)\mathbf{g}}, \quad (35)$$

and it occurs when $\mathbf{g} \cdot \boldsymbol{\varphi}$ is an integer multiple of 2π , i.e., when

$$q\varphi_2 - p\varphi_1 = 2\pi n \quad (36)$$

with n being any integer. Assuming that φ_1 and φ_2 satisfy this condition of maximum resonance, from equation (24) together with $v_{-\mathbf{k}} = v_{\mathbf{k}}$, it follows that

$$\bar{V}_T(\boldsymbol{\Omega}_0 + \delta\boldsymbol{\omega}, \boldsymbol{\varphi}) \sim 2 \sum_{\ell=0}^{\infty} v_{(2\ell+1)\mathbf{g}} \text{sinc}[(2\ell+1)T\mathbf{g} \cdot \delta\boldsymbol{\omega}], \quad (37)$$

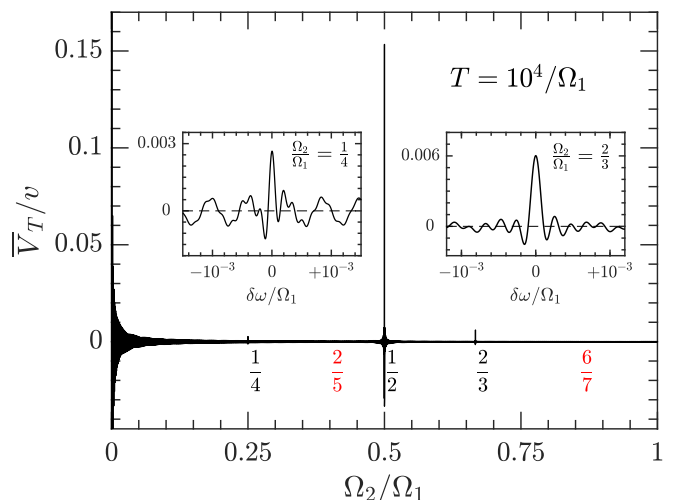


Fig. 1. Dependence of the dimensionless average velocity \bar{V}_T/v on Ω_2/Ω_1 for $A_1 = A_2 = 1$, $\varphi_1 = \varphi_2 = 0$, and $T = 10^4/\Omega_1$. The resonance peaks corresponding to the fractions 0 (only partially shown for better visibility of the remaining peaks) and 1/2 are clearly visible. The ones corresponding to 1/4 and 2/3 are also visible but considerably smaller. Other resonances, such as the ones corresponding to 2/5 and 6/7 shown in Figure 3 cannot be appreciated on this scale. The insets show a zoomed-in view around $\Omega_2/\Omega_1 = 1/4$ (left inset) and $\Omega_2/\Omega_1 = 2/3$ (right inset) in terms of $\delta\omega/\Omega_1 = \Omega_2/\Omega_1 - p/q$.

provided that $|\delta\boldsymbol{\omega}| = \mathcal{O}(T^{-1})$ and that T is large enough such that the term R_T can be neglected. Note that, in this case, $\bar{V}_T(\boldsymbol{\Omega}_0 + \delta\boldsymbol{\omega}, \boldsymbol{\varphi})$ vanishes whenever $\mathbf{g} \cdot \delta\boldsymbol{\omega}$ is a nonzero integer multiple of π/T . Thus, if we set $\delta\omega_1 = 0$ and vary $\delta\omega_2$, $\bar{V}_T(\boldsymbol{\Omega}_0 + \delta\boldsymbol{\omega}, \boldsymbol{\varphi})$ vanishes when $\delta\omega_2$ is a nonzero integer multiple of $\pi/(qT)$, whereas if we set $\delta\omega_2 = 0$ and vary $\delta\omega_1$, $\bar{V}_T(\boldsymbol{\Omega}_0 + \delta\boldsymbol{\omega}, \boldsymbol{\varphi})$ vanishes if $\delta\omega_1$ is a nonzero integer multiple of $\pi/(pT)$.

To illustrate our theoretical results, we have calculated $\bar{V}_T(\boldsymbol{\Omega}, \boldsymbol{\varphi})$ using equation (10) with $\bar{Q}_T(\boldsymbol{\Omega}, \boldsymbol{\varphi}) = \bar{V}_T(\boldsymbol{\Omega}, \boldsymbol{\varphi})$, and $q_{\mathbf{k}}(\boldsymbol{\Omega}) = v_{\mathbf{k}}$. The coefficients $v_{\mathbf{k}}$ appearing in that equation have been evaluated using equation (34). To ensure that both drivings have roughly the same influence, we have focused on the most symmetric case of equal driving amplitudes. Specifically, in all the figures of this section we have taken $A_1 = A_2 = 1$. In addition, to maximize the height of the resonance peaks, we have restricted our analysis to values of φ_1 and φ_2 that satisfy the condition of maximum resonance in equation (36).

In Figure 1, we plot the dimensionless time-average velocity \bar{V}_T/v as a function of Ω_2/Ω_1 for $\varphi_1 = \varphi_2 = 0$ and $T = 10^4/\Omega_1$. According to our theoretical results, there should emerge resonance peaks when Ω_2/Ω_1 is equal to a rational number. Furthermore, only the resonances corresponding to the fractions 0, 1/4, 1/2, and 2/3 are visible. Other resonances, such as the ones corresponding to 2/5 and 6/7 studied below, cannot be appreciated in the figure. This absence of resonances is not due to the use of a finite averaging time. In fact, these peaks would be imperceptible even in the limit $T \rightarrow \infty$, because they are

very small compared to the smallest peak visible in Figure 1. Indeed, using equation (35), it is easy to verify that at $\Omega_2/\Omega_1 = 1/4$ (the smallest peak visible in Figure 1), $\bar{V}_{\infty, M}$ is approximately equal to $3 \times 10^{-3}v$, whereas at $\Omega_2/\Omega_1 = 2/5$ and $\Omega_2/\Omega_1 = 6/7$, $\bar{V}_{\infty, M}$ is approximately equal to $7 \times 10^{-5}v$ and $7 \times 10^{-11}v$, respectively.

To analyze in more detail the behavior of \bar{V}_T in the vicinity of a (q, p) -resonance, we now consider that one frequency, say Ω_1 , is kept fixed, while the other frequency, Ω_2 , is varied around the value $p\Omega_1/q$. In terms of our previous notation, this corresponds to setting $\delta\omega_1 = 0$ and $\delta\omega_2 = \Omega_2 - p\Omega_1/q$. Henceforth, for notational simplicity, we will write $\delta\omega$ instead of $\delta\omega_2$. In addition, to facilitate comparison with the asymptotic expression (37), we will use the dimensionless variable $q\delta\omega T$, which here is nothing but $T\mathbf{g} \cdot \delta\boldsymbol{\omega}$.

In Figures 2 and 3, we depict the dependence of \bar{V}_T/v on $q\delta\omega T$ for the resonances $(q, p) = (4, 1)$ (left column in Figure 2), $(q, p) = (3, 2)$ (right column in Figure 2), $(q, p) = (5, 2)$ (left column in Figure 3), and $(q, p) = (7, 6)$ (right column in Figure 3). To analyze how these peaks emerge as the averaging time increases, different values of T have been considered, which are indicated in the panels. In addition, in each panel, q curves have been plotted, corresponding to the values $\varphi_2 = 2\pi n/q$, with $n = 0, \dots, q-1$. Since $\varphi_1 = 0$, all these values satisfy the condition of maximum resonance in equation (36). The results in Figures 2 and 3 corroborate the theoretical prediction that, for sufficiently large values of T , the q curves converge to the asymptotic result in equation (37). Surprisingly, the averaging times necessary to reach the asymptotic regime are huge in comparison to the period of the driving $\mathcal{T} = 2\pi q/\Omega_1$.

6 Quantum mechanical two-level system

Let us now consider a dissipative quantum mechanical model with the Hamiltonian $H(t) = H_0 + H_D(t)$, where

$$H_0 = \frac{\epsilon}{2}(\sigma_x \cos \theta + \sigma_z \sin \theta) \quad (38)$$

and the bichromatic driving

$$H_D(t) = A_1 \sigma_x \cos(\Omega_1 t + \varphi_1) + A_2 \sigma_z \cos(\Omega_2 t + \varphi_2). \quad (39)$$

To ensure that both drivings have roughly the same impact, we focus on the most symmetric case $\theta = \pi/4$ and equal driving amplitudes, $A_1 = A_2 \equiv A$.

For the consideration of dissipation, one may start from a system-bath model to obtain an equation of motion for the reduced density operator of the dissipative system. Then one can show that generally dissipation is quantitatively affected by the driving [25, 26]. Here however, we are interested in the generic response to bichromatic drivings and, thus, we follow a less involved path which allows an efficient numerical solution for rather long propagation

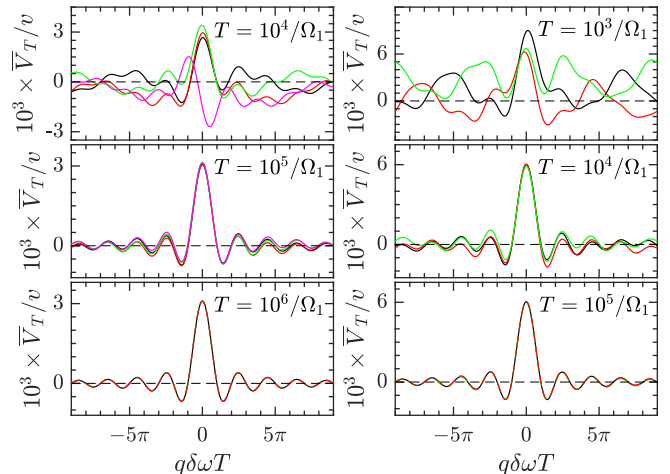


Fig. 2. Dependence of the dimensionless average velocity \bar{V}_T/v on the dimensionless variable $q\delta\omega T$ for the resonances $(q, p) = (4, 1)$ (left column) and $(q, p) = (3, 2)$ (right column), and the values of the averaging times displayed in the panels. For all the curves $\varphi_1 = 0$ and $A_1 = A_2 = 1$. In each panel, there are q curves corresponding to the values $\varphi_2 = 2\pi n/q$, for $n = 0, \dots, q-1$, which are obtained from the condition of maximum resonance in equation (36). As expected from the theoretical analysis, with increasing the value of T , the q curves converge to the asymptotic curve given by equation (37).

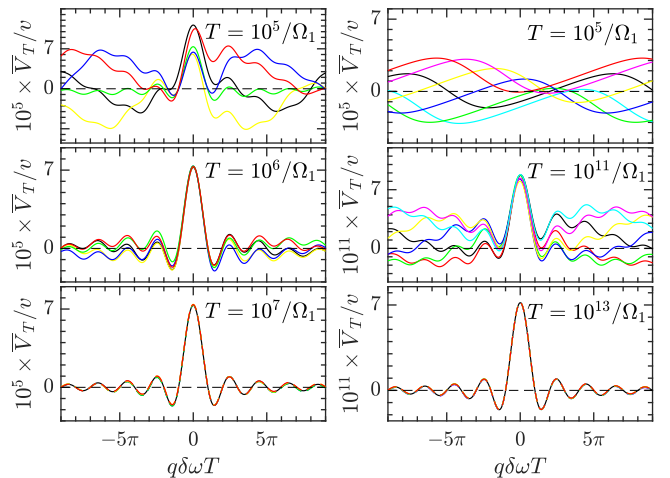


Fig. 3. The same as in Figure 2 but for the resonances $(q, p) = (5, 2)$ (left column) and $(q, p) = (7, 6)$ (right column).

times. In doing so, we employ a Lindblad master equation for the density operator [27], $\dot{\rho} = -i[H_0 + H_D(t), \rho] + \gamma\mathcal{D}(\rho)$ (in units with $\hbar = 1$) with a dissipator [27]

$$\mathcal{D}\rho = \tilde{\sigma}_- \rho \tilde{\sigma}_+ - \frac{1}{2} \tilde{\sigma}_+ \tilde{\sigma}_- \rho - \frac{1}{2} \rho \tilde{\sigma}_+ \tilde{\sigma}_-, \quad (40)$$

where $\tilde{\sigma}_- = |\varphi_0\rangle\langle\varphi_1| = \sigma_+^\dagger$ induces dissipative decay from the excited state $|\varphi_1\rangle$ of the undriven Hamiltonian H_0 to the corresponding ground state $|\varphi_0\rangle$.

As an observable Q , we may choose any combination of Pauli matrices. Generic features, however, will not depend on the particular choice such that without loss of

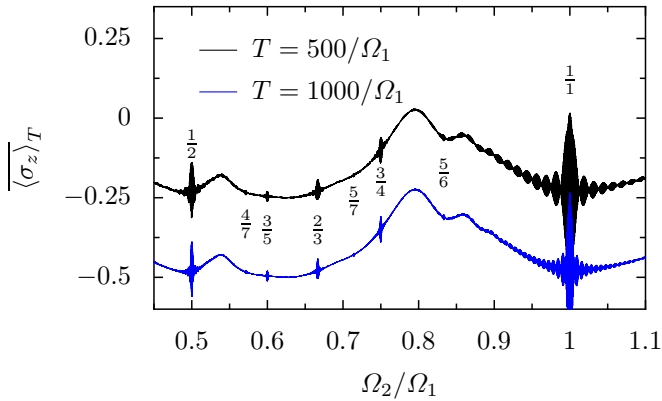


Fig. 4. Time-averaged response of the bichromatically driven two-level system after a transient stage averaged over various times T . When Ω_2/Ω_1 is close to a rational p/q , peaks with generic shape emerge (labeled by the corresponding fraction). Parameter values are: $\epsilon = \sqrt{2}\Omega_1$, $\theta = \pi/4$, $A_1 = A_2 = \Omega_1$, and $\gamma = 0.2\Omega_1$. For graphical reasons, the curve for $T = 500/\Omega_1$ is vertically shifted.

generality, we consider $Q_t^{\text{st}} \equiv \langle \sigma_z \rangle_t$. To ensure independence of details, we have verified all numerical results by using also slightly different setups and observables.

We start by sketching the global picture of the response (Figure 4) which shows $\langle \sigma_z \rangle_T$ for two different averaging times T as a function of Ω_2 and for various phases φ_2 (in this section, we always take $\varphi_1 = 0$). As expected, $\langle \sigma_z \rangle_T$ exhibits resonance peaks at simple rational values of Ω_2/Ω_1 which sharpen with increasing T . The size of the peaks as well as the shape of the background depend on details. Generally it is such that the (1,1) resonance is rather prominent, which can be understood by frequency mixing: For two equal driving frequencies, a zero-frequency response can be obtained already in second-order perturbation theory. For all other values of (q, p) , one has to go to higher order. Henceforth we focus on the universal features in narrow regions around pronounced peaks.

As smaller peaks tend to be less compromised by components with $\ell \neq 1$, we study the emergence of a peak with increasing propagation time T for $(q, p) = (5, 3)$. Figure 5 shows $\langle \sigma_z \rangle_T$ for the 20 equally spaced phases $\varphi_2 = 2\pi n/20$ with $n = 0, 1, \dots, 19$. For the relatively short propagation time $T = 150/\Omega_1$, all curves are significantly different from each other, while a clear peak structure is still missing. With increasing T and staring at the center $\delta\omega = 0$, curves for phases that differ by $2\pi/q$ coincide, such that eventually $20/q = 4$ groups of curves emerge. This reflects the $2\pi/q$ periodicity in φ_2 derived above for $\delta\omega = 0$. Moreover, it confirms the generalization conjectured from equation (24), namely that the periodicity to a good approximation holds in a whole neighborhood of the (q, p) -peak.

To underline this result, we also plot the curves within one $2\pi/q$ period and those for φ_2 equal to multiples of $2\pi/q$ separately, but now for the $(q, p) = (7, 5)$ resonance, see Figure 6. The left column contains the results for values of φ_2 in the range $[0, 2\pi/q]$. They show that only for a

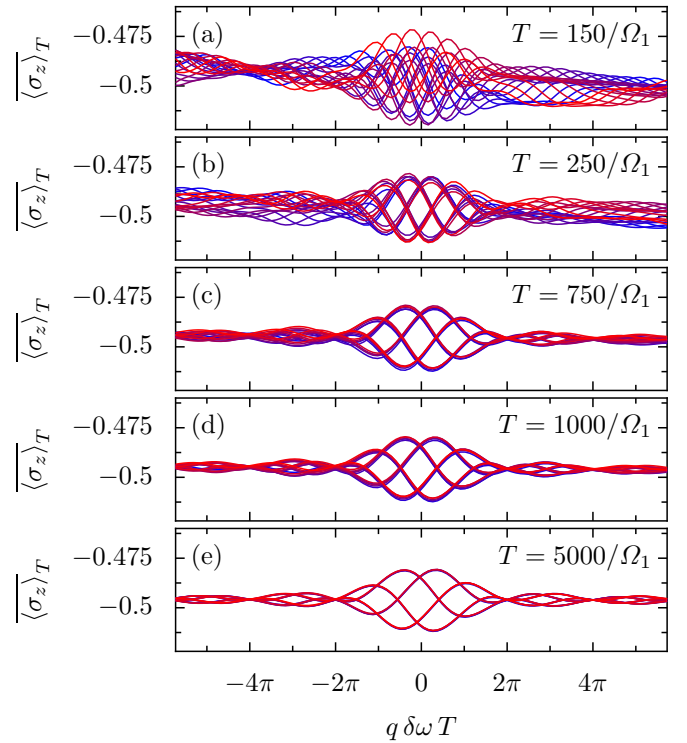


Fig. 5. Resonance peak $(q, p) = (5, 3)$ for the phases $\varphi_1 = 0$ and $\varphi_2 = 2\pi n/(4q)$, with $n = 0, 1, \dots, 4q - 1$, showing the transition from 2π -periodicity to $2\pi/q$ -periodicity. Notice that the abscissa is scaled with the averaging time T . All other parameters are as in Figure 4.

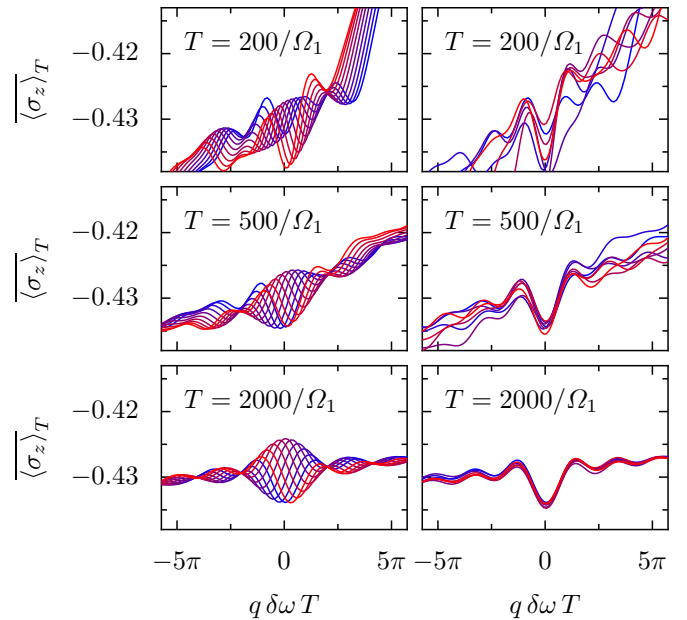


Fig. 6. Resonance peak $(q, p) = (7, 5)$ for the averaging times displayed in the graphics, while all other parameters are as in Figure 4. Left column: Result for 10 equally spaced phases $\varphi_2 = 2\pi n/(10q)$ for $n = 0, 1, \dots, 9$ showing that for sufficiently large T , the curve for $\varphi_2 = 0$ ($n = 0$, blue) smoothly connects to the one for $\varphi_2 = 2\pi/q$. Right column: The same but for $\varphi_2 = 2\pi n/q$, $n = 0, 1, \dots, q - 1$. With increasing T , the curves start to coincide.

sufficiently large T , the enveloping function is dominated by the $\ell = 1$ component and resembles the sinc conjectured in equation (24). Moreover, the first and the last curve smoothly connect to each other, which depicts how the $2\pi/q$ -periodicity emerges. Accordingly, the curves for φ_2 at multiples of $2\pi/q$ eventually coincide, as can be appreciated in the right column of Fig. 6

As a remnant of finite propagation time T , we witness in all panels of Figure 6 an inclination of the resonance peak, which to a smaller extent is noticeable also in Figure 5. It stems from the global background of $\langle \overline{\sigma_z} \rangle_T$ visible in Figure 4. Owing to the scaling of the abscissa, it diminishes with increasing T and, in accordance with equation (24), it eventually vanishes.

7 Conclusions

We have studied the asymptotic limit of multichromatically driven, dissipative dynamical systems. It turned out that a strict distinction between commensurable and incommensurable frequencies requires an infinite propagation time. Nevertheless, there exists a noticeable difference between the two cases, namely that only for commensurable frequencies the phases of the driving fields may matter. Moreover, the phase dependence generally has a lower periodicity than the naively expected 2π . While this implies non-generic features of the resonances, the resulting peaks upon variation of the phase exhibit a generic form given by sinc functions.

While the limiting behavior can be derived analytically, we have performed numerical studies to see how the limits are approached. For a classical random walk on a lattice with bichromatically time-dependent transition rates, the velocity has been obtained analytically up to the numerical computation of a sum. The response as a function of the two driving frequencies shows how resonances emerge around rational values of Ω_2/Ω_1 .

The case of a dissipative two-level system has been treated fully numerically. It revealed how with increasing propagation time, the generic features of resonance peaks emerge, namely the sinc shape and the sub 2π periodicity in the phase shift. The width of the resonance peaks at rational frequency quotients shrinks with increasing averaging time, such that the background eventually appears flat and the peaks become pronounced. The value of the response depends on the relative phase of the two drivings, while in its vicinity, the response becomes phase independent.

An important point in practical calculations is that commensurable frequency ratios with rather large numerator or denominator imply large periods. Then owing to the necessarily finite propagation time, this periodicity may still not be manifest in the result. In other words, up to such finite time, the system behaves as if it were quasi-periodic, i.e., as if the frequencies were incommensurable. However, in particular for the random-walk model, it may take even considerably longer until the peaks assume their generic shape. Quantitative statements about this issue still represent a challenge for future investigations.

This work was supported by the Spanish Ministry of Science, Innovation, and Universities through the CSIC Research Platform on Quantum Technologies PTI-001 and via grants No. MAT2017-86717-P and FIS2017-86478-P.

References

1. L. Gammaitoni, P. Hänggi, P. Jung, F. Marchesoni, *Rev. Mod. Phys.* **70**, 223 (1998)
2. J. Casado-Pascual, J. Gómez-Ordóñez, M. Morillo, P. Hänggi, *Phys. Rev. Lett.* **91**, 210601 (2003)
3. V. Anishchenko, A. Neiman, A. Astakhov, T. Vadiavasova, L. Schimansky-Geier, *Chaotic and Stochastic Processes in Dynamic Systems* (Springer, Berlin, 2002)
4. J.A. Freund, L. Schimansky-Geier, P. Hänggi, *Chaos* **13**, 225 (2003)
5. B. Lindner, J. Garcia-Ojalvo, A. Neiman, L. Schimansky-Geier, *Phys. Rep.* **392**, 321 (2004)
6. J. Casado-Pascual, J. Gómez-Ordóñez, M. Morillo, J. Lehmann, I. Goychuk, P. Hänggi, *Phys. Rev. E* **71**, 011101 (2005)
7. I. Goychuk, J. Casado-Pascual, M. Morillo, J. Lehmann, P. Hänggi, *Phys. Rev. Lett.* **97**, 210601 (2006)
8. P. Reimann, *Phys. Rep.* **361**, 57 (2002)
9. P. Hänggi, F. Marchesoni, *Rev. Mod. Phys.* **81**, 387 (2009)
10. D. Cubero, F. Renzoni, *Brownian Ratchets: From Statistical Physics to Bio and Nano-motors* (Cambridge University Press, Cambridge, 2016)
11. S. Flach, O. Yevtushenko, Y. Zolotaryuk, *Phys. Rev. Lett.* **84**, 2358 (2000)
12. D. Cubero, F. Renzoni, *Phys. Rev. E* **97**, 062139 (2018)
13. D. Cubero, G.R. Robb, F. Renzoni, *Phys. Rev. Lett.* **121**, 213904 (2018)
14. J. Casado-Pascual, D. Cubero, F. Renzoni, *Phys. Rev. E* **88**, 062919 (2013)
15. J. Casado-Pascual, J.A. Cuesta, N.R. Quintero, R. Alvarez-Nodarse, *Phys. Rev. E* **91**, 022905 (2015)
16. P. Reimann, M. Grifoni, P. Hänggi, *Phys. Rev. Lett.* **79**, 10 (1997)
17. J. Lehmann, S. Kohler, P. Hänggi, A. Nitzan, *J. Chem. Phys.* **118**, 3283 (2003)
18. S. Kohler, J. Lehmann, P. Hänggi, *Phys. Rep.* **406**, 379 (2005)
19. F. Forster, M. Mühlbacher, R. Blattmann, D. Schuh, W. Wegscheider, S. Ludwig, S. Kohler, *Phys. Rev. B* **92**, 245422 (2015)
20. S. Platonov, B. Kästner, H.W. Schumacher, S. Kohler, S. Ludwig, *Phys. Rev. Lett.* **115**, 106801 (2015)
21. S. Morito, H.M. Salkin, *Fibonacci Quart.* **17**, 361 (1979)
22. S. Morito, H.M. Salkin, *Acta Inform.* **13**, 379 (1980)
23. N.G. van Kampen, *Stochastic processes in physics and chemistry* (North-Holland, Amsterdam, 1992)
24. P. Hänggi, P. Talkner, M. Borkovec, *Rev. Mod. Phys.* **62**, 251 (1990)
25. S. Kohler, T. Dittrich, P. Hänggi, *Phys. Rev. E* **55**, 300 (1997)
26. M. Grifoni, P. Hänggi, *Phys. Rep.* **304**, 229 (1998)
27. H.P. Breuer, F. Petruccione, *Theory of Open Quantum Systems* (Oxford University Press, Oxford, 2003)